

---

## Biweekly current oscillations on the continental slope of the Gulf of Guinea

Annick Vangriesheim<sup>a\*</sup>, Anne Marie Treguier<sup>b</sup> and Gael Andre<sup>c</sup>

<sup>a</sup>Laboratoire Environnement Profond, Ifremer, Brest, France

<sup>b</sup>Laboratoire de Physique des Océans, CNRS-Ifremer-UBO, Brest, France

<sup>c</sup>Laboratoire Physique Hydrodynamique et Sédimentaire, Ifremer, Brest, France

\*: Corresponding author : Tel.: +33 2 98 22 42 98; fax: +33 2 98 22 47 57. [annick.vangriesheim@ifremer.fr](mailto:annick.vangriesheim@ifremer.fr)

---

**Abstract:** Current meter measurements have been carried out for 3 years on the continental slope of the Gulf of Guinea, near 7.5°S off the Angola coast. Currents in a water depth of 1300 m over the continental slope show a remarkable biweekly oscillation, bottom intensified, and with currents oriented nearly parallel to the isobaths. With a peak-to-peak amplitude reaching 20–30 cm/s, this signal is the most energetic at sub-inertial frequencies. Simultaneous measurements deeper on the continental rise (in a water depth of 4000 m) show a more complex signal dominated by lower frequencies, and with less clear polarization. Simple linear topographic wave theories are compared to the observations. A combination of coastal trapped waves with cross-slope mode 3–5 could be consistent with the observed currents. A three-dimensional 1/6° composite function (small circle) model suggests the existence of modes trapped to the slope, although with lower amplitude than observed.

**Keywords:** Continental slope / Current oscillation / Current meter measurement / Linear wave model

# Biweekly current oscillations on the continental slope of the Gulf of Guinea

Annick Vangriesheim \*

*DRO/EP, Ifremer, Brest, France*

Anne Marie Treguier

*Laboratoire de Physique des Océans, CNRS-Ifremer-UBO, Brest, France*

Gael Andre

*DEL/AO, Ifremer, Brest, France*

---

## Abstract

Current meter measurements have been carried out for three years on the continental slope of the Gulf of Guinea, near  $7.5^{\circ}\text{S}$  off the Angola coast. Currents in a water depth of 1300 m over the continental slope show a remarkable biweekly oscillation, bottom intensified, and with currents oriented nearly parallel to the isobaths. With a peak-to-peak amplitude reaching 20-30 cm/s at 30 meters above the bottom, this signal is the most energetic at sub-inertial frequencies. Simultaneous measurements deeper on the continental rise (in a water depth of 4000 m) show a more complex signal dominated by lower frequencies, and with less clear polarization. Simple linear topographic wave theories are compared to the observations. A combination of coastal trapped waves with cross-slope mode 3 to 5 could be consistent with the observed currents. A three-dimensional  $1/6^{\circ}$  model suggests the existence of modes trapped to the slope, although with lower amplitude than observed.

---

## 1 Introduction

In the framework of the French multi-disciplinary BIOZAIRE program conducted by IFREMER in the Gulf of Guinea, several long-term moorings were installed near

---

\* Corresponding author.

*Email address:* annick.vangriesheim@ifremer.fr (Annick Vangriesheim).

the seabed between years 2000 and 2003. The purpose of these moorings equipped with sediment traps and current meters was to study the amount and the variability of the organic material supply for the benthic organisms living in the sediment, in a deep ocean area from around 1300 m on the slope to around 4000 m off the Angola coast (Fig. 1). A striking feature of the current meter measurements on the continental slope on the 1300 m isobath is a biweekly oscillation that dominates the low-frequency signal (after filtering out tidal and inertial motions). Oscillations at periods between one week and one month have been frequently observed on continental slopes near the bottom, but it is quite remarkable that at site A of BIOZAIRE those oscillations stand out as the most energetic low frequency signal. At other locations in the deep ocean, (e.g., Uheara et al., 2000) such oscillations correspond to a spectral peak but do not dominate the time series, due to the larger variability present in the mesoscale band (periods of one month to one year).

Because of their dominant contribution to the total current fluctuations, biweekly oscillations as observed at site A control the variability of other parameters such as temperature, and could influence the benthic biology. It is thus important to document their characteristics as observed from the current meter data, which is done in the present paper.

Oscillations at periods close to 13-15 days have been described previously in the Gulf of Guinea from temperature and sea level measurements, but not in deep water. Most observations were located on the shelf in the northern part of the Gulf of Guinea, where the coast is oriented zonally (Picaut and Verstraete, 1979; Garzoli, 1987). Picaut and Verstraete (1979) found two peaks in the series of sea surface height at two tidal periods: 13.66 days (Mf, lunar fortnightly tide) and 14.76 days

(Msf, luni-solar fortnightly tide). Because the astronomic forcing at the Msf periods is very weak, they concluded that the oscillations observed at this period were likely due to a non-linear interaction between M2 and S2 semi-diurnal tides. The signal propagated polewards along the coast with a velocity of 54 cm/s. Clarke and Battisti (1983) tried to interpret these observations in terms of free, linear coastal trapped waves. They could not draw firm conclusions because of limitations in their model (which only resolved the gravest modes) and the lack of observations on the slope and in the deep ocean.

In this paper we use a similar approach to interpret our new measurements off the Angola coast, using linear wave theory (coastal trapped waves but also Kelvin waves and topographic Rossby waves). Interpretation of our observationnal results is hampered by the fact that the measurements were not designed to study such waves: many aspects of the theories cannot be verified using our limited dataset. A  $1/6^\circ$  model of the Atlantic circulation (Treguier et al., 2003) is used in an attempt to supplement the observationnal information. Although its resolution is not adequate to represent faithfully the observed currents near the bottom, this model does help to bridge the gap between data and theory.

## **2 Data**

The BIOZAIRE multi-disciplinary program investigated conditions at different sites from the continental slope to the abyssal plain of the Gulf of Guinea off the Angola coast (Fig. 1). The current data analysed in the present work are those from the so-called site A in a water depth of about 1300 m and those from site C near

4000 m. The moorings, lasting approximately one year, were installed three times at the same locations between 2000 and 2003. At each site, two levels above the bottom were studied: 30 meters above the bottom (mab hereafter) and 410 mab. Two additional levels were instrumented in 2000 at site A: 10 and 150 mab. Due to failures or to fouling, data gaps are present in some time series. Fig. 2 shows the periods and depths of the available data. The Aanderaa RCM8 instruments used in the observation program were pre-calibrated at the Ifremer laboratories. In this work, we focus on the oscillations of intermediate periods (a week to a month). Short periods (tidal, inertial gravity band) and seasonal to interannual variability will be discussed elsewhere.

For a first look at the results, some statistics are presented in Table 1. At site A, there is a definite mean current towards the south, which seems bottom-intensified with values between 1 and 2  $\text{cm}\cdot\text{s}^{-1}$  at 30 mab. The mean zonal velocity is more variable from year to year and particularly as a function of depth, but it is always smaller than the mean meridional velocity. A mean current toward the south-east is consistent with the expected residual circulation (Mercier et al., 2003). The eddy kinetic energy does not decrease towards the bottom but rather is bottom-intensified in some years (2001, for instance). At the deeper site C, the mean velocity is smaller, but the southeastward orientation of the mean currents is similar to Site A. The eddy kinetic energy is smaller at site C (5 to 7  $\text{cm}^2\cdot\text{s}^{-2}$ ) than at site A (around 30  $\text{cm}^2\cdot\text{s}^{-2}$ ).

The time series display variability at a variety of time scales with the spectral content varying substantially between locations. Semi-diurnal oscillations are present at both sites and inertial oscillations are well developed at site C (period  $\approx 90\text{h}$ )

whereas they are not so energetic at site A (period  $\approx 94\text{h}$ ). To filter this high frequency variability, a low-pass filter has been used : a Lanczos filter with a cut-off period (i.e. half power point) of 6 days. In Fig. 3, where the three filtered time series for site A are joined end to end, a very obvious oscillation is seen with greater amplitude and more definite polarization at 30 mab than at 410 mab. The direction of this oscillation is almost parallel to the local isobaths. The direction "along" the bathymetry, found empirically using a detailed plot of the bathymetry (Fig.4), is  $27^\circ$  from North counterclockwise. The progressive vector diagrams at site A during the first leg in 2000 for three depths (150 mab, 30 mab and 10 mab) are shown in Fig. 5. One notices that at 150 mab, the current orientation exhibits somewhat more variability than at the deeper levels, where the direction is also closer to the bathymetry orientation. At site C deeper on the continental rise (Fig. 6), the stick plots have a very different character. The current variability is more random, and no single frequency dominates the signal in the range of one week to one year. No preferred direction emerges either, and the bottom intensification is less marked than at site A.

Kinetic energy spectra have been computed for the longest time series at the two sites (Figs. 7b and 7c). For site A, time series are available at three depths during year 2000 (150 mab, 30 mab and 10 mab): they are plotted in Fig. 7a to allow investigation of the vertical structure of the variability. At site A, peaks appear at a period close to 15 days for all levels. They are of the same order of magnitude at 150, 30 and 10 mab in 2000 but smaller at 410 mab when available (2001 and 2002, Fig. 7b). A smaller peak appears also near a period of 30 days at 410 and 30 mab (Figs. 7b and 7c). Spectral analysis provides the orientations of the current ellipses

and the principal axes for the 15 day period at site A (Fig. 8a). The ellipses confirm the bottom-intensification between 410 and 30 mab and the stronger polarization near the bottom in the direction parallel to the bathymetric contours. We have estimated the coherence on the vertical at site A for the currents parallel to the isobaths. Along-slope currents at 10 mab, 30 mab and 150 mab (year 2000) and at 30 mab and 410 mab (years 2001 and 2002) are coherent vertically at the 95% confidence level for the periods near 15 days and 30 days. However, the phase lag varies from year to year.

An oscillation with period close to 15 days is also observed in the temperature time series at site A, with an amplitude of 0.1 to 0.2°C (Fig. 9). The temperature fluctuations seem similar to the velocity fluctuations, but the phase shift between temperature and velocity does not seem stationary. At site C, temperature oscillations are very small.

The contrast between the nature of the variability observed at sites A and C clearly stands out in Figs. 7 and 8. At site C, the variability is greatest around the 30 day period and the main axis of the ellipse is not oriented along the topography for the measurements closest to the bottom.

We note that site A is right on the slope whereas site C is located at the foot of the rise. The difference in bottom slope between the two sites probably plays an important role in determining the nature of the enhanced current variability for periods near 15 days at site A.

### 3 Linear wave models

Numerous measurements on continental slopes have shown oscillations at periods of 10 to 40 days that have been attributed to linear vorticity waves (see for example Mysak (1980) for a review). The restoring force for those waves is the vortex stretching due to the topographic slope. Quite interestingly, the literature about vorticity waves falls into two classes. On one hand, measurements made in deep water (1000 m or more) have been interpreted as plane topographic Rossby waves (for example, Johns and Watts, 1986, or Uehara and Miyake, 2000). On the other hand, measurements made on the continental shelf or on the upper portion of the continental slope have been interpreted in terms of coastal trapped waves (for example, Brink, 1982, Clarke and Battisti, 1983, or Middleton and Wright, 1991). Both models represent vorticity waves above a topographic slope, but they differ by their respective boundary conditions.

The plane topographic Rossby wave (Rhines, 1970) is an extension of the classical Rossby wave, taking into account the topographic slope rather than the planetary  $\beta$  effect as a restoring force. Using the quasigeostrophic approximation, the wave modes can be completely described by a streamfunction  $\psi(x, y, z, t)$ . Here, we follow Rhines (1970) and consider a solution that is linearized about a resting ocean with uniform stratification  $\partial\rho/\partial z$ , Brunt-Vaisala frequency  $N$  and uniform depth  $H$ . The Coriolis frequency  $f_0$  is constant; the topographic slope  $\Gamma$  is assumed to be constant and infinite in extent. We consider plane wave solutions with horizontal wavenumber  $\mathbf{K} = (k, l)$ :

$$\Psi(x, y, z, t) = F(z)e^{i(kx+ly-\omega t)}. \quad (1)$$

Without loss of generality we assume that  $x$  is the cross-slope direction (the topography does not vary as a function of  $y$ ). The vertical structure function  $F$ , proportional to  $\cosh(|\mathbf{K}|Nz/f_0)$ , is bottom-intensified. The wave frequency is given by the dispersion relation

$$\omega = \Gamma N \sin \theta \coth\left(\frac{|\mathbf{K}|NH}{f_0}\right), \quad (2)$$

where  $\theta$  is the angle that the wave vector makes with the downslope direction. The waves propagate with shallow water to their left (right) in the southern (northern) hemisphere. In the limit of short wavelength compared to the Rossby radius, the dispersion relation is approximately  $\omega = \Gamma N \sin \theta$ ; low frequency waves ( $\sin \theta \approx 0$ ) tend to have a wavevector aligned with the cross-slope direction, which means that the currents tend to be aligned with the bathymetry. For a monochromatic topographic Rossby wave, velocities are in phase on the vertical. Temperature oscillations are in quadrature with the velocity  $v$  along the bathymetric contours, because temperature oscillations are proportional to  $\partial\psi/\partial z$  and  $v = \partial\psi/\partial x$ , with  $\psi$  defined by (1).

The geometry of an infinite, uniformly sloping bottom does not apply well to the continental slope, where the ocean depth  $H$  varies enormously over a narrow region of a few hundreds of kilometers. Nevertheless, Johns and Watts (1986) have found good agreement between the quasigeostrophic linear theory and the properties of 40-day oscillations measured between 2000 and 4000m depth below the Gulf Stream, on the American continental slope. However, the linear topographic wave that fit their measurements had a cross-slope wavelength of 130 km, which is not small compared to the total width of the continental slope at that location (about

300 km) so that the hypothesis of an infinite slope must be questioned.

The finite extent of the continental slope is an essential ingredient of the coastal trapped wave (CTW) theory, as presented for example by Huthnance (1978). The simplest theory is inviscid and considers a semi-infinite domain bounded at the coast at  $x = 0$ , with a uniform stratification  $N(z)$  and a topography that is a function only of the cross-shore direction  $h(x)$ . The linear solutions are waves propagating in the along-shore ( $y$ ) direction. They have a fixed cross-slope modal structure, function of  $x$  and  $z$ . The solutions depend on the Burger number

$$Bu = \frac{N^2 H^2}{f_0^2 L^2}, \quad (3)$$

where  $L$  is the typical width of the slope. In the limit of small  $Bu$  (low stratification) solutions are barotropic Kelvin waves and shelf waves. For very large  $Bu$ , the Rossby radius is large compared to the width of the slope and solutions are similar to internal Kelvin waves, propagating with the coast to the left in the southern hemisphere. At large wavenumber, bottom-trapped modes similar to the topographic Rossby waves are recovered. One key aspect of the theory is that because of the imposed boundary conditions at  $x = 0$  and  $x = \infty$ , individual modes do not propagate up or down the slope. Observations of cross-slope phase propagation (as in Johns and Watts, 1986) can be reconciled with the theory only by a sum of modes. A similar, more familiar problem arises when describing the ocean using vertical baroclinic modes: more than one mode is needed to reproduce an upward (or downward) phase propagation.

Brink and Chapman (1987) have written a numerical algorithm which calculates the frequency as well as the vertical and cross-slope structure of CTWs, given a

stratification  $N(z)$  and an arbitrary cross-slope structure  $h(x)$ . A single equation for pressure  $P$  can be derived,

$$\frac{\partial}{\partial t} \left( \frac{\partial^2 P}{\partial x^2} + \frac{\partial^2 P}{\partial y^2} \right) + \left( f^2 + \frac{\partial^2}{\partial t^2} \right) \left( \frac{\partial^2}{\partial z \partial t} \frac{1}{N^2} \frac{\partial P}{\partial z} \right) = F. \quad (4)$$

For a given along-shore wavenumber  $k$ , the resonant frequencies are found by solving iteratively the equation for arbitrary forcing  $F$  and varying the frequency.

Using the Brink and Chapman program we have calculated dispersion relations for the free modes at the latitude of BIOZAIRE using the local topography. The Vaisala frequency has been evaluated using the climatology of Reynaud et al.(1998) averaged between 8°S and 7°S and 8°E and 12°E. The profile (not shown) has a sharp thermocline with an average value  $N = 0.017 \text{ s}^{-1}$  in the first 100 m. The average over the water depth (4000 m) is  $N = 0.002 \text{ s}^{-1}$ . The corresponding Rossby radii in deep water (4000 m) are 122.7, 62.9 and 42.5 km for the first three baroclinic modes. The corresponding flat-bottom Kelvin wave speeds are 2.3, 1.2 and 0.8 m/s. The model is two-dimensional: no variation of the bathymetry in the along-shore direction is allowed, and the  $\beta$  effect is neglected. We have used a topographic profile which is the average of 10 cross-slope profiles in a box of size 300 km around site A. The solution of (4) is obtained numerically using finite differences in a  $\sigma$  (bottom-following) coordinate system. Our implementation of the Brink and Chapman model includes 101 grid points with a grid spacing of 5 km and 201  $\sigma$  levels. We assume no bottom friction.

Sensitivity experiments show that the model results are dependent on the structure of the topography (replacing the realistic bathymetry by a linear slope modifies significantly the phase speed of the waves). Extending the model domain changes

the phase speeds by a few percents, without affecting the structure of the modes.

Dispersion relations are shown for the first 5 modes in Fig.10. The corresponding dispersion relations for flat-bottom, deep ocean Kelvin waves (depth of 4000 m) are indicated by dashed lines. Because of the low latitude and the strong stratification, the Burger number  $Bu$  is large (using the vertical average of the Vaisala frequency  $N$ ,  $Bu = 4.8$ ). This explains the similarity between the Coastal Trapped Waves and baroclinic Kelvin waves at low frequency. For the period of the motions observed during BIOZAIRE (15 days), solutions exist at wavelengths of 3600 km and smaller (table 2), depending on the mode number.

Examples of the structure of two cross-shelf modes are shown in Fig.11. The mode number corresponds to the number of zero-crossings for the along-slope velocity. The structure is slanted over the topography and decays away from the bottom. As in the theory of topographic Rossby waves over an infinite slope, higher modes (higher wavenumbers) are more bottom-trapped. Note that the cross-slope velocity is smaller than the along-slope velocity by almost one order of magnitude.

Clarke and Battisti (1983) have used the same model to calculate the characteristics of mode 1 and mode 2 coastal trapped waves near  $5^{\circ}\text{N}$  along the northern coast of the Gulf of Guinea. They find much lower phase speeds than ours for the 15 days period (1.3 m/s for mode 1 and 0.64 m/s for mode 2). The  $\beta$  effect slows down the waves in their case due to the West-East orientation of the coast, but by 20% only. Differences may be due to the different profiles of the bathymetry at the two locations. They may also have to do with numerical inaccuracy (at the time of Clarke and Battisti's study, the model could use only 17 equally spaced grid points on the vertical, which is not enough to capture the thin thermocline).

## 4 Model-data comparison

For a detailed interpretation of data in terms of topographic Rossby waves or coastal trapped waves, many moorings are necessary to determine the along-slope and cross-slope variations in the wave. The biozaire measurements were not made for that purpose: only one mooring is available on the slope (site A) and another one at the bottom of the slope, approximately along the same cross-slope axis (site C). Besides the dominant frequency of the oscillatory motions, the useful elements for a comparison with theory are the bottom intensification of the motions and the orientation of the currents with respect to the topographic slope.

Topographic Rossby waves have a uniform bottom intensification with exponential decay rate  $z_d = KN/f_0$ . In the North Pacific around  $41^\circ\text{N}$ , Uehara and Miyake (2000) have used this property to estimate a wavenumber  $K$  from the observed bottom intensification of their bi-weekly oscillations. Their mooring was in a water depth of 3500 m, with current meters at 500 m and 2500 m above bottom, respectively. The authors found that the corresponding wavelength varied from 100 km to 506 km between years (they had 5 years of moorings at the same location). They interpreted the discrepancies between theoretical and observational results to be a consequence of the Oyashio current, a current which sometimes penetrates to great depths. They concluded that there was a part of the variability they observed which could not be explained by linear topographic Rossby waves.

There is no strong mean current at the location of the BIOZAIRE moorings, and because of the closeness of the equator we may expect a more linear regime. However, our attempts to fit plane topographic Rossby waves to our data following

Uehara and Miyake (2000) are not conclusive. The observations summarized in table 3 show a modest intensification of the currents at site A between 150 mab and 30 mab, but a larger one (factor of 4 to 10) between 410 mab and 30 mab. The bottom intensification of plane topographic Rossby waves depends on the stratification. According to our choice of a constant  $N$  (taking either its value at 1300m, or a value representative of the deeper ocean) the observed intensification could fit topographic Rossby waves of 150 to 300 km wavelength, which leaves a factor of two uncertainty. The theory of plane topographic Rossby waves has recently been extended to the case of an exponentially varying stratification  $N$ , more appropriate to the tropical ocean (Reid and Wang, 2004). Using such a model would remove some of the arbitrariness in the choice of  $N$ . However the dispersion diagram is not very different from the case of a constant stratification in the case of a small  $kl$  ratio, which is relevant to our observations.

For wavelengths of 150 to 300 km at a period of 15 days, the theoretical angle between the major axis of the current ellipses and the topography is  $\theta = 13^\circ$  to  $30^\circ$ , much larger than observed (see table 3). Uehara and Miyake (2000) also find discrepancies between the theoretical angle and their observations. We thus proceed to consider the coastal trapped waves description which makes fewer approximations and fully takes into account the finite variation in ocean depth.

For inviscid CTW, velocities are in quadrature and current ellipses are aligned exactly with the topography. This characteristic is in rough agreement with the observations: the angle between the major axis of the current ellipses and the along-slope direction is a few degrees only (table 3). The vertical structure of energy is more complicated than for the case of plane Rossby waves because it varies a lot with the

position on the slope. An intensification close to 1 between 30 mab and 150 mab, and factor of 4-10 between 30 mab and 410 mab, are compatible either with mode 3 or mode 5. To further discriminate the modes, we note that the time series at site A (1300 m depth) and site C (4000 m depth) at 30 mab have a significant coherence at a period of 15 days, with a small lag ( $7^\circ$ ). For mode 3 (Fig. 11), the oscillations at 4000 m depth and 1300 m depth are out of phase (a lag of  $180^\circ$ ), while for mode 5 they are in phase, which fits the observations better.

The fit between observations and the mode 5 CTW is far from perfect. In the case of an inviscid, linear mode, along-slope and cross-slope velocities are exactly in quadrature and there is no phase shift between different locations. This is not the case in the observations. The presence of friction could introduce phase shifts in each mode (Brink, 1990), but it seems that the observations cannot be explained in terms of a single mode. Observations show oscillations at different periods (15 days to 30 days) and it is likely that different spatial scales (or different CTW modes) are present. This is also suggested by the lack of a well defined phase relationship between the current meter measurements at different depths: at site A the coherence between the series is significant at the 95% confidence level for the 15 days period, but there is a phase shift of 30 to  $65^\circ$  which varies from year to year. A monochromatic Rossby wave or a single CTW mode would result in zero phase change in the vertical direction. Similarly, we have noted in section 2 that the temperature measurements display oscillations at the 15 days period with some coherence with the velocity oscillations (Fig. 9), but the phase shift is not reliable from one year to the next.

To investigate the matter further, we have considered the results of a fully three

dimensional, primitive equation model of the Atlantic circulation called ATL6. This model has been implemented in the context of the French CLIPPER project and is described in Treguier et al., 2003. ATL6 has a  $1/6^\circ$  grid size, 42 levels in the vertical with grid spacing varying between 12 m at the top to 200 m at the bottom. It uses standard "z" coordinates, which means that the bathymetry is represented as a series of steps. The model is forced by daily winds and fluxes of the ECMWF center: the ERA15 reanalysis for years 1979-1993, and the analysis for years 1994-2000. First, we have considered daily model output at the location of site A (Roy, 2002). The model shows little bottom intensification of currents. There are peaks in the spectrum at frequencies of 15 and 30 days, but the 15-day frequency is less energetic than the 30-day one, and model velocities near the bottom are lower than observed velocities by a factor of 5 to 10. This could be due to insufficient vertical and horizontal resolution. At 1300m depth, the model has a vertical grid spacing of 200m, which is not suitable to represent bottom-trapped motions. With a  $1/6^\circ$  horizontal grid, the width of the continental slope at site A is less than 20 grid points, which is barely sufficient to represent the first three CTW modes.

Despite these shortcomings, the model velocity in the BIOZAIRE area displays variability trapped along the slope. The structure of the along-slope velocity shown in Fig. 12 has some similarities with a mode 4 CTW. An animation of this section shows that the variability does not correspond to a single CTW; different modes seem to dominate the signal at different times. Fig 13b is a time series of the bottom along-slope velocity on the section during year 2000. The structure is often, but not always, similar to a mode 3 CTW. Sometimes variability seems in phase across the slope, but sometimes there is upwards (eastwards) phase propagation. One key

difference between this model solution and CTW linear modes is the westward propagation at all vertical levels, which is prominent when one looks at animations of model velocity away from the slope. An indication of westward propagation is found in Fig 13a which represents the meridional velocity at a fixed depth. In the three-dimensional model, energy is not confined to the slope but is able to propagate into the interior (as Rossby waves, for instance).

In principle, model results could help us understand how CTWs are forced. The ATL6 model variability in the tropics is generated by the atmospheric forcing, but also by instabilities of the main currents. One example is the meanders of the Equatorial undercurrent, at periods of 15 days to one month (Arhan et al., 2004). We think however that the ATL6 model is not well suited to study in more detail the source of the bottom-trapped variability because its grid is too coarse. We plan to use a higher resolution regional model to investigate this question further.

## **5 Discussion**

Three years of current meter measurements on the African continental slope near 7.5 °S have shown the existence of bottom-trapped oscillations at a dominant period of 15 days. The direction of these currents is closely aligned with the local bathymetry. The amplitude of the oscillations near the bottom (30 mab) reaches 20-30 cm/s and dominates the observed variability after filtering out inertial oscillations and tides. The current time series are quite different at a nearby site situated at the bottom of the slope. This has led us to investigate whether the oscillations on the slope are topographic waves.

Linear theory shows that topographic Rossby waves and Coastal Trapped Waves (CTW) exist at a period near 15 days. A monochromatic Rossby wave is not consistent with the measurements, and neither is one single CTW mode. The Rossby wave model cannot explain both the large bottom intensification and the small angle between currents and topography at site A. Furthermore, the hypothesis of a wavelength small compared to the horizontal scale of the topographic slope is not satisfied. A superposition of coastal trapped waves of modes 3 to 5 with wavelengths 680 to 1200 km in the along-slope direction could perhaps explain the observations. The simple CTW model considered here has severe limitations, though. For example, it does not allow the radiation of Rossby waves westward into the interior of the basin, a feature which is important in the three-dimensional model ATL6.

The dispersion relations of both topographic Rossby waves and CTWs allow free waves at all frequencies lower than inertial, as the along-slope wavenumber varies continuously. In the absence of any narrow resonance phenomenon, one wonders why the 15 days period is so energetic in the response: does it result from geometric constraints selecting wavenumbers, or does it result from the forcing mechanism?

Previous authors have observed oscillations at these time-scales on slope margins (Brink et al., 1980; Picaut, 1984; Shumann and Brink, 1990; Uehara et al., 2000, and others). In the northern Gulf of Guinea, those oscillations have been attributed to tidal forcing (Picaut and Verstraete, 1979; Garzoli, 1987). Picaut and Verstrate invoked a nonlinear interaction between M2 and S2 semi-diurnal tides. They suggested that the signal could be generated in the North-East corner of the Gulf of Guinea where the shelf is wider, and then propagate westward along the Northern

coast.

In the part of the Gulf of Guinea where the present data come from, there is no previous study performed with current measurements. We have examined time series of sea level measured at Pointe Noire ( $4^{\circ} 48'S$ ) and Luanda ( $8^{\circ} 47'S$ ) during the seventies and the eighties. Those series are archived jointly by the University of Hawaii Sea Level Center and the U.S. National Oceanographic Data Center. Spectra reveal significant peaks at a period between 13 and 15 days. Only one peak is found, in contrast with the results of Picaut and Verstraete (1979) for the record from Abidjan, but this could be due to the short duration of our series (3.5 years at most). The peak could correspond to the period of the Mf tide (13.66 days), but nonlinear mechanisms would be needed to explain the generation of strong currents over the slope at that frequency (the Mf tide has a very large scale, and no significant propagation in the Gulf of Guinea).

The winds could also force a 15 days response. Grodsky and Carton (2001) showed that the zonal wind component over the Gulf of Guinea near the Equator has a bi-weekly oscillation which is related to the rainfall. We have examined wind stress series measured by the Quikscat scatterometer and available at the CERSAT archival center. Spectra of the wind stress at the location of site A for years 2000 to 2003 show energy at periods near 15 days, but the spectra are rather white and the 15 day period does not dominate the signal as is the case in the bottom currents. The same is true for a wind stress time series from near the equator.

Because Site A is quite close to the equator, we believe that the generation of topographic waves along the slope cannot be understood as a quasi two-dimensional problem (like the simple linear Coastal Trapped Wave model used here). An inves-

tigation of the forcing mechanisms requires a high resolution, three dimensional model of the Gulf of Guinea, which we are planning to build.

### **Acknowledgements**

We thank our IFREMER colleagues: Myriam Sibuet who was the chief scientist of the BIOZAIRE project, and Alexis Kripounoff, Philippe Crassous and Jean-Pierre Brulport who were in charge of the mooring experiments. Ken Brink and Bernard Le Cann helped us with the coastal trapped wave model and the interpretation of its results. We thank TOTAL for its financial participation in the BIOZAIRE project. The CLIPPER ATL6 model was run at the IDRIS computer center in Orsay, France. The CLIPPER project is funded by various French government agencies: CNRS, IFREMER, CMO, CNES and Meteo-France.

### **References**

- Arhan, M., A.M. Treguier, B. Bourles, 2004: Diagnosing the annual cycle of the Equatorial undercurrent in the Atlantic Ocean in a general circulation model. Manuscript in preparation.
- Brink, K. H., D. Halpern and R. L. Smith, 1980: Circulation in the Peruvian upwelling system near 15°S. *J. Geophys. Res.*, **85**, 4036-4048.
- Brink, K.H, 1982: A comparison of long coastal trapped wave theory with observations off Peru. *J. Phys. Oceanogr.*, **12**, 897-913.
- Brink, K.H, and D.C. Chapman, 1987: Program for computing properties of coastal-trapped waves and wind driven motions over the continental shelf

- and slope, second edition. Woods Hole Oceanographic Institution Tech. Rep., WHOI-87-24, 119p.
- Brink, K.H., 1990: On the Damping of free coastal-trapped waves. *J. Phys. Oceanogr.*, **20**, 1219-1225.
- Chelton, D.B., R.A. deSzoeke, and M.G. Schlax, 1998: Geographical Variability of the First Baroclinic Rossby Radius of Deformation. *J. Phys. Oceanogr.*, **28**, 433-460.
- Clarke, A.J., and D. S. Battisti, 1983: Identification of the fortnightly wave observed along the Northern Coast of the Gulf of Guinea. *J. Phys. Oceanogr.*, **13**, 2192-2200.
- Huthnance, J.M., 1975: On trapped waves over a continental shelf. *J. Fluid Mech.*, **69**, 686-704.
- Huthnance, J.M., 1978: On coastal trapped waves: analysis and numerical calculation by inverse iteration. *J. Phys. Oceanogr.*, **8**, 74-93.
- Johns, W.E., and D.R. Watts, 1986: time scales and structure of topographic Rossby waves and meanders in the deep Gulf Stream. *J. Mar. Res.*, **44**, 267-290.
- Mercier, H., M. Arhan, and J.R.E. Lujtjeharms, 2003: Upper-layer circulation in the eastern equatorial and the South Atlantic ocean in january-march 1995. *Deep Sea Res.*, I, 50, 863-887.
- Middleton, J.F., and D. G. Wright, 1991: coastal-trapped waves on the Labrador shelf. *J. Geophys. Res.*, **96**, 2599-2617.
- Mysak, A., 1980: Topographically trapped waves. *J. Fluid. Mech.*, **12**, 45-76.
- Picaut, J., 1984: On the dynamics of thermal variations in the Gulf of Guinea. *Oceanogr. trop.*, **19**, 127-153.
- Picaut J. et Verstraete J.M., 1979: Propagation of a 14.7 day wave along the northern

- coast of the Guinea Gulf. *J. Phys. Oceanogr.*, **9**, 136-149.
- Pedlosky, J., 1979: Geophysical fluid dynamics. *Springer-Verlag*, 624 p., 408-416.
- Reid, R.O. and O. Wang, 2004: Bottom-trapped Rossby waves in an exponentially stratified ocean. *J. Phys. Oceanogr.*, **34**, 961-967.
- Reynaud, T., P. Legrand, H. Mercier and B. Barnier, 1998: A new analysis of hydrographic data in the Atlantic and its application to an inverse modelling study. *WOCE newsletter*, **32**, 29-32.
- Rhines, P.B., 1970: Edge-, Bottom-, and Rossby waves in a rotating stratified fluid. *Geophys. Fluid Dyn.*, **1**, 273-302.
- Roy, A., 2002: Modélisation des courants profonds: interprétation des données courantométriques. Report from the Institut Supérieur d'Informatique de Modélisation et de leurs Applications (ISIMA), 60 pp.
- Schumann, E.H., and K. H. Brink, 1990: Coastal-trapped waves off the coast of South Africa: Generation, propagation and current structures. *J. Phys. Oceanogr.*, **20**, 1206-1217.
- Treguier, A. M., O. Boebel, B. Barnier, and G. Madec, 2003: Agulhas eddy fluxes in a  $1/6^\circ$  Atlantic model. *Deep Sea Res.*, II, **50**, 251-280.
- Uehara K. et Miyake H., 2000: Biweekly periodic deep flow on the slope inshore of the Kuril-Kamchatka trench. *J. Phys. Oceanogr.*, **30**, 3249-3260.

<b>Location</b>	<b>Year</b>	$\bar{u}$ (cm.s <sup>-1</sup> )	$\bar{v}$ (cm.s <sup>-1</sup> )	$KE$ (cm <sup>2</sup> .s <sup>-2</sup> )
<b>Site A</b>				
410 mab	2001	-0.2	-0.4	16.6
	2002	-0.1	-0.4	20.9
150 mab	2000	0.8	-1.1	44.2
30 mab	2000	1.7	-2.7	42.8
	2001	0.5	-1.4	27.6
	2002	0.6	-1.9	20.5
10 mab	2000	0.6	-2.0	22.3
<b>Site C</b>				
410 mab	2001	0.5	-0.5	4.6
	2002	0.1	-0.1	3.3
30 mab	2000	0.3	0.0	2.1
	2001	0.7	-1.7	3.7
	2002	-0.1	-1.0	2.9

Table 1

Current Statistics at sites A and C. The mean velocity in the zonal direction ( $\bar{u}$ ) and the meridional direction ( $\bar{v}$ ) are indicated, as well as the eddy kinetic energy of the filtered time series (cut-off period of 6 days, see text). Only results corresponding to time series longer than 250 days are shown here.

mode	wavelength (km)	phase velocity $\text{m.s}^{-1}$
1	3694	2.84
2	1795	1.39
3	1232	0.94
4	938	0.72
5	679	0.52
6	571	0.44

Table 2

Characteristics of the first 6 modes of coastal trapped waves for the computed period closest to 15 days

Year	mab	Period (days)	Energy ratio	Orientation Degree
2000	30, 150	14.5-17.5	1. - 1.7	0-3
2001	30, 410	13-16.5	6. - 10.	1-8
2002	30, 410	14-15.5	4. - 10.	3-5

Table 3

Period of spectral peak, energy ratio, and orientation of the current ellipses with respect to the topography, measured at site A. The energy ratio is between the two different depths indicated in mab (meters above bottom). The ranges indicated are the maximum and minimum among values found by using four different definitions of the frequency bands (averages over 3, 4, 5 and 6 neighbouring frequencies)

## List of Figures

1	General view of the region and the mooring locations.	26
2	Duration of the time series. The depth is indicated in meters above bottom (mab). The total depth is about 1300 m at site A and 4000 m at site C. The dates of the beginning and end of each time series is indicated, as well as the duration of the interruption between two consecutive mooring series (in hours or in days). The duration of each current meter record is indicated in days.	27
3	Stick plots of velocities at site A. Top: 410 mab; bottom: 30 mab.	28
4	Direction of the topographic slope at site A. Contour interval 200m.	29
5	Progressive vector diagram of velocities at site A during the year 2000 deployment, at 150, 30 and 10 meters above bottom (mab). The direction North is indicated, as well as the direction parallel to the isobaths (thin arrow).	30
6	Stick plots of velocities at site C. Top: 410 mab; bottom: 30 mab.	31
7	Kinetic energy spectra. a, Three different depths at site A during year 2000. b, two different depths at site A for years 2001 and 2002. c, two different depths at site C for years 2001 and 2002.	33
8	Variance ellipses for filtered series in the frequency band around 15 days. The directions parallel and perpendicular to the topography are indicated by dashed lines. a) and b): years 2000 and 2002 at site A, c): year 2002 at site C.	35
9	Filtered time series of the velocity in the direction of the bathymetric contours, and the temperature anomaly relative to the mean ( $4.22^{\circ}$ ). The data are from the first two current meter deployments (from March 2000 to September 2001) at 30 mab at site A.	36

- 10 Dispersion relation for the first 5 modes of coastal trapped waves in the BIOZAIRE area (solid curves). For each mode, the dashed line represents the dispersion relation of a flat bottom Kelvin wave (4000 m depth). The period  $2\pi/\sigma = 15$  days is indicated by a horizontal line. 37
- 11 Spatial structure of the perturbation of along-shore velocity  $V$  and cross-shore velocity  $U$  for coastal trapped wave modes 3 and 5. Velocities are rescaled so that the maximum of  $V$  is one; note that  $U$  is multiplied by 10 to be plotted with the same color scale. The zero contour is indicated by the thick line. Crosses indicate the location of mooring C (near 4000 m) and mooring A (near 1300 m). 38
- 12 Meridional velocity at  $7.3^\circ\text{S}$  in the ATL6 model (m/s), averaged over 5 days (14-19 August 2000). Each colored box is a model grid cell. Contours are from  $-0.05 \text{ m}\cdot\text{s}^{-1}$  to  $0.05 \text{ m}\cdot\text{s}^{-1}$  by  $0.01 \text{ m}\cdot\text{s}^{-1}$ . The zero contour is indicated in bold. Black crosses note the approximate location of moorings A and C. 39
- 13 Time-series of meridional velocity along the slope at  $7.3^\circ\text{S}$  in the ATL6 model (m/s), for year 2000, from the 5-days averaged model output. A black line is drawn at the approximate location of site A (site C is at the western boundary of the plot). Top panel: velocity in model layer 17 (572 m depth). Bottom: velocity in the model bottom layer. 40

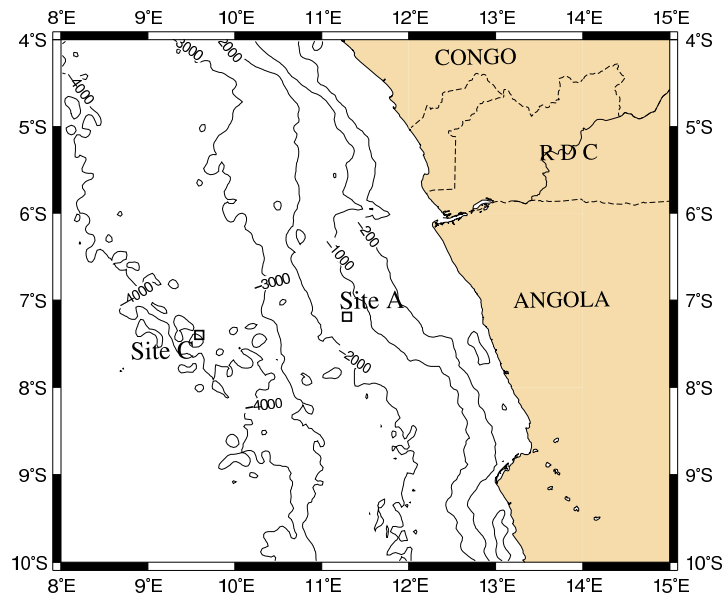


Fig. 1. General view of the region and the mooring locations.

	MAB	2000	2001	2002	2003
Site A	410	03/27 — 70d — 06/05 [216d]	01/07 — 315d — 11/19 [58h] — 11/21	438d	02/03
	150	03/27 — 284d	01/05		
	30	03/27 — 284d — 01/05 [45h]	01/07 — 250d — 09/15 [67d] — 11/21	438d	02/03
	10	03/27 — 284d	01/05		
Site C	410		01/08 — 319d — 11/24 [12h]	434d	02/02
	30	03/31 — 282d	01/08 [10h] — 319d — 11/24 [12h]	434d	02/02

Fig. 2. Duration of the time series. The depth is indicated in meters above bottom (mab). The total depth is about 1300 m at site A and 4000 m at site C. The dates of the beginning and end of each time series is indicated, as well as the duration of the interruption between two consecutive mooring series (in hours or in days). The duration of each current meter record is indicated in days.

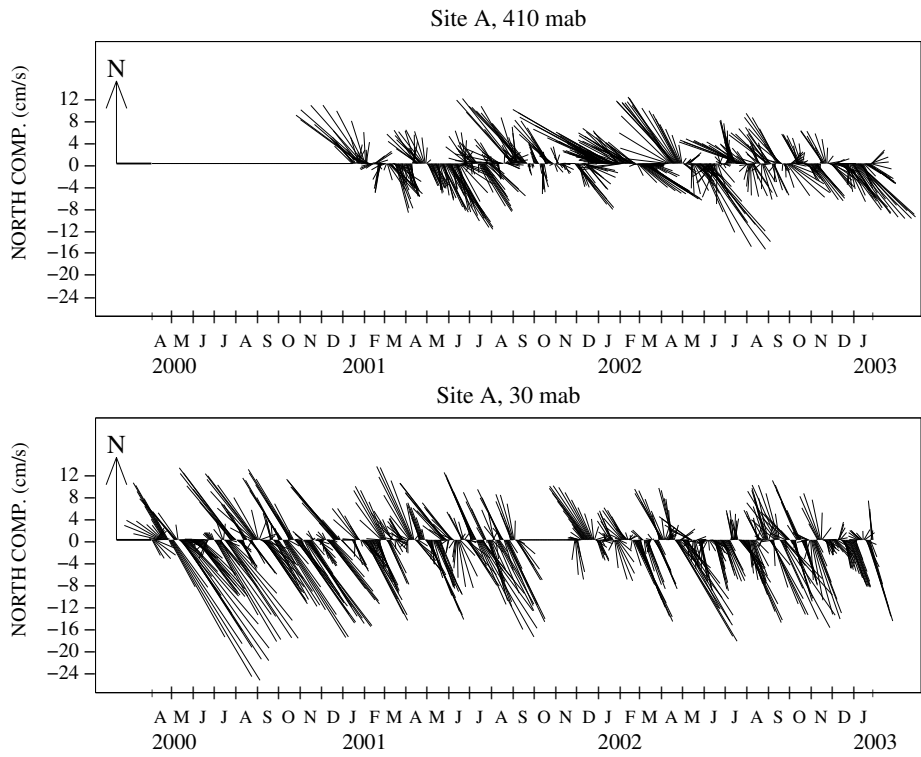


Fig. 3. Stick plots of velocities at site A. Top: 410 mab; bottom: 30 mab.

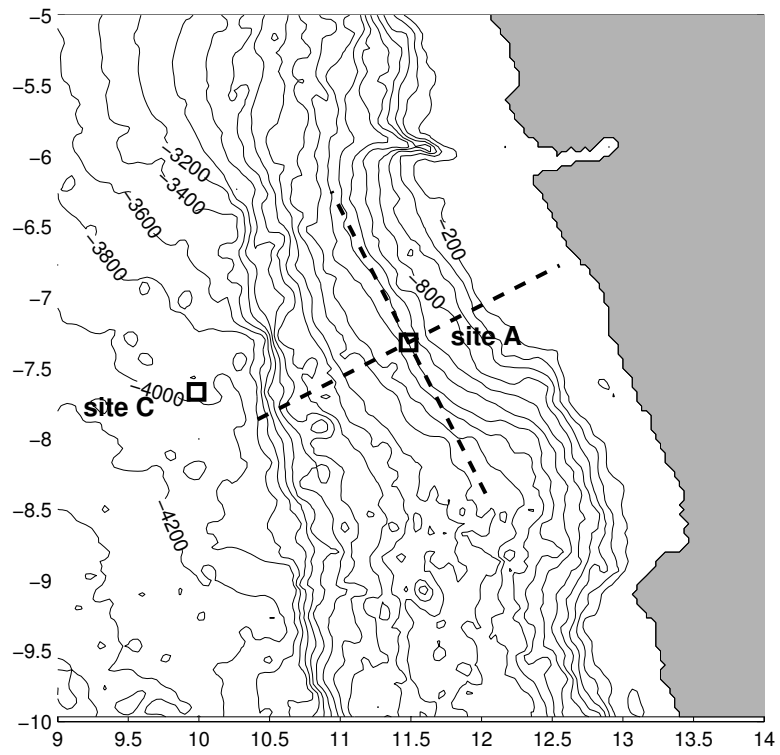


Fig. 4. Direction of the topographic slope at site A. Contour interval 200m.

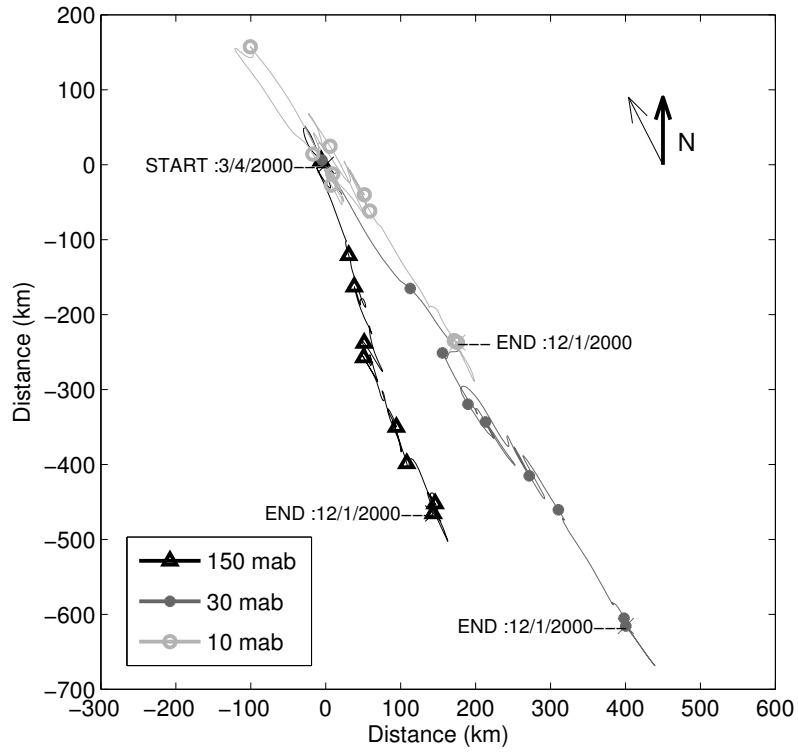


Fig. 5. Progressive vector diagram of velocities at site A during the year 2000 deployment, at 150, 30 and 10 meters above bottom (mab). The direction North is indicated, as well as the direction parallel to the isobaths (thin arrow).

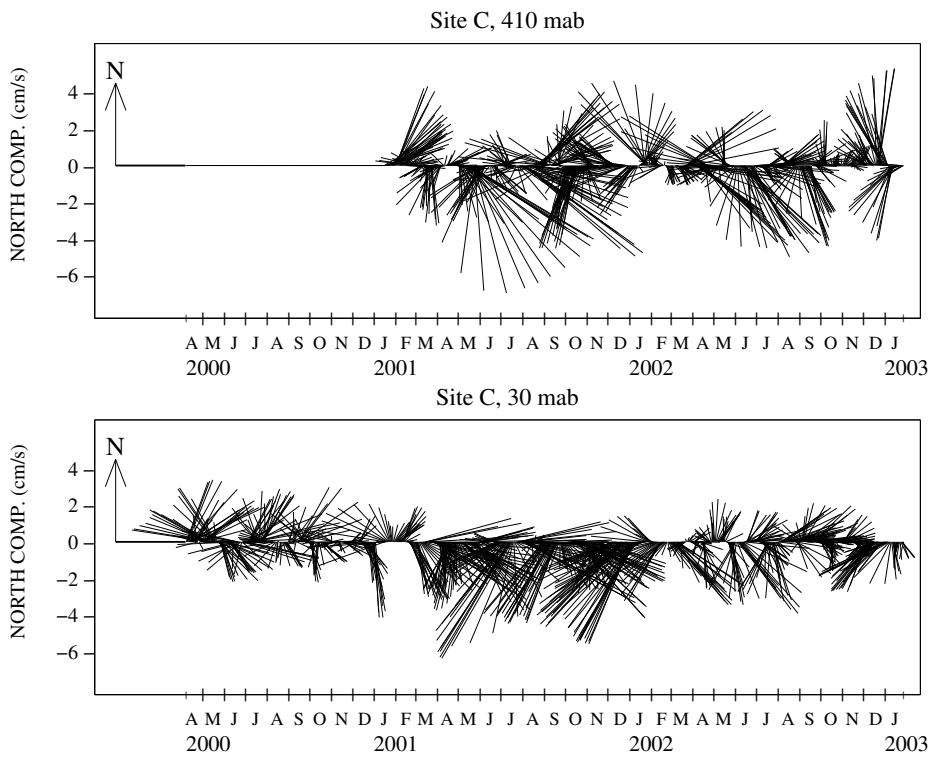
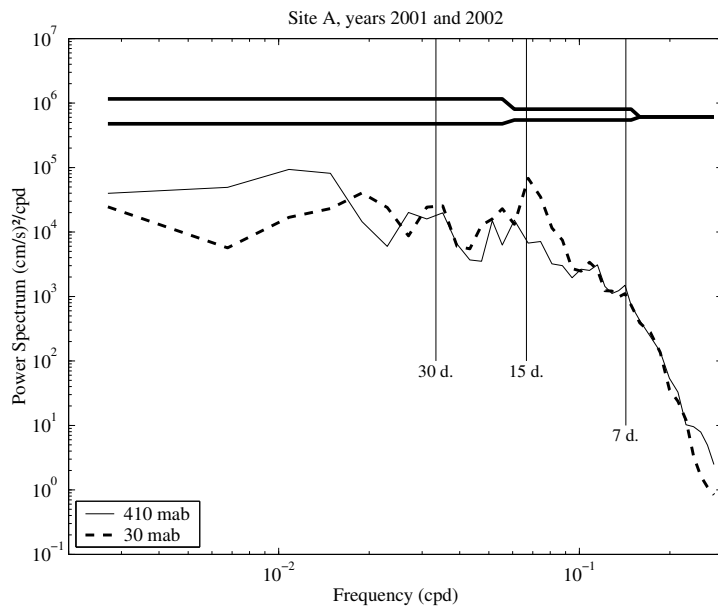
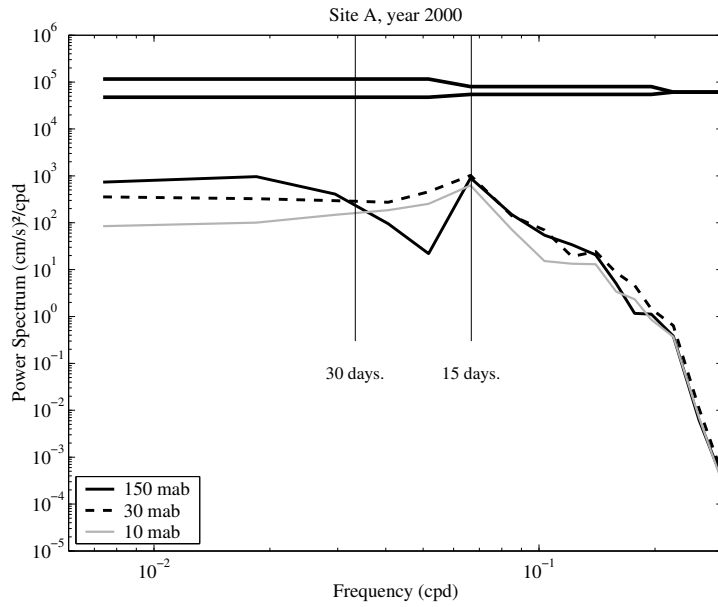


Fig. 6. Stick plots of velocities at site C. Top: 410 mab; bottom: 30 mab.



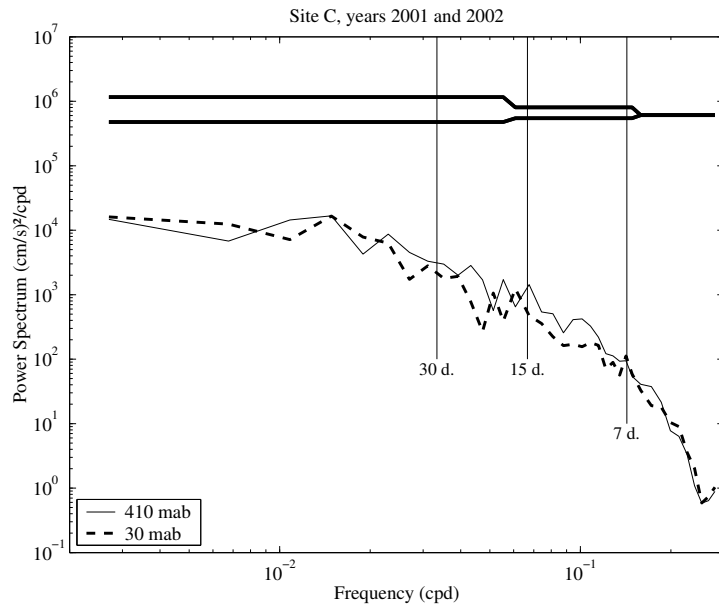
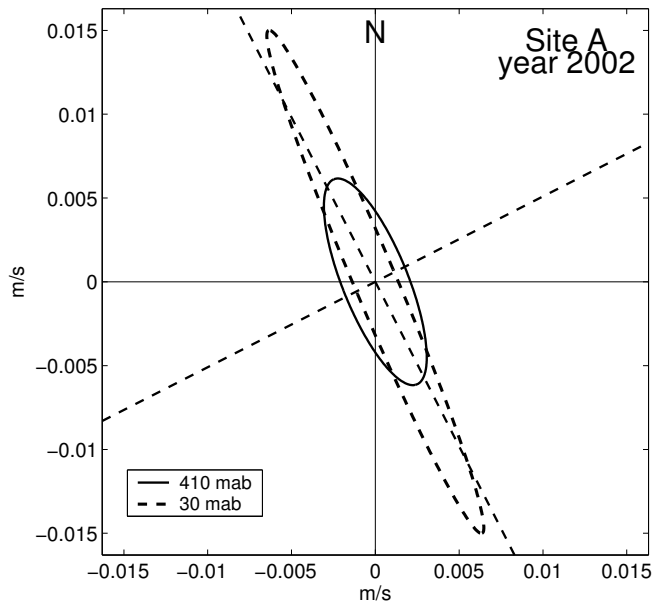
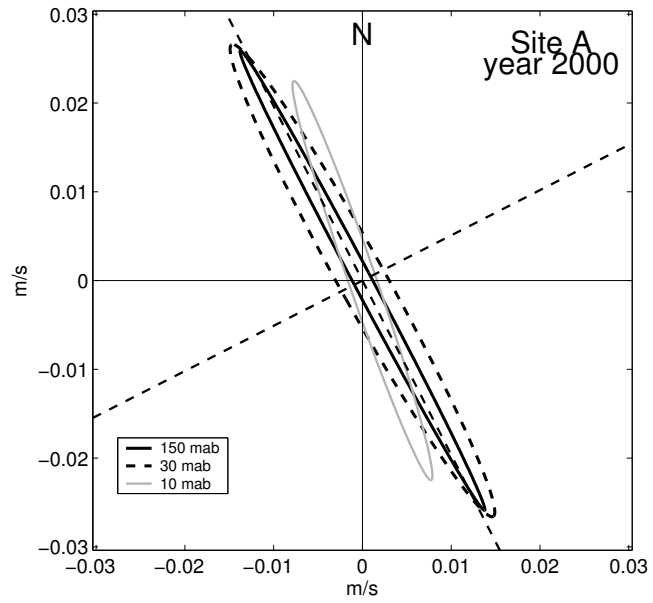


Fig. 7. Kinetic energy spectra. a, Three different depths at site A during year 2000. b, two different depths at site A for years 2001 and 2002. c, two different depths at site C for years 2001 and 2002.



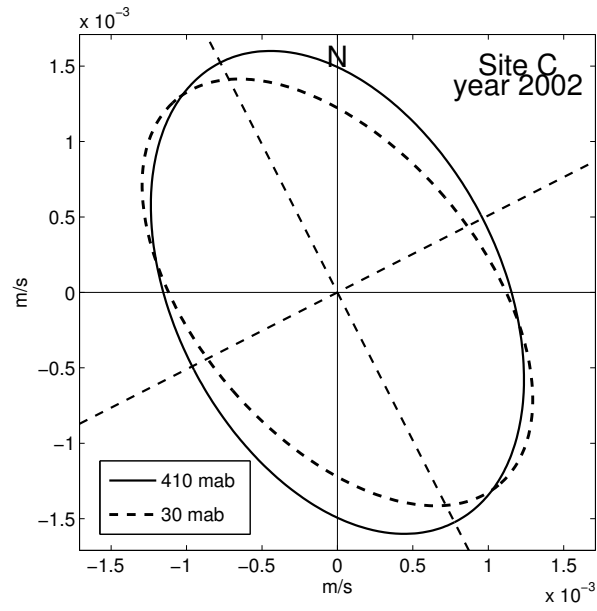


Fig. 8. Variance ellipses for filtered series in the frequency band around 15 days. The directions parallel and perpendicular to the topography are indicated by dashed lines. a) and b): years 2000 and 2002 at site A, c): year 2002 at site C.

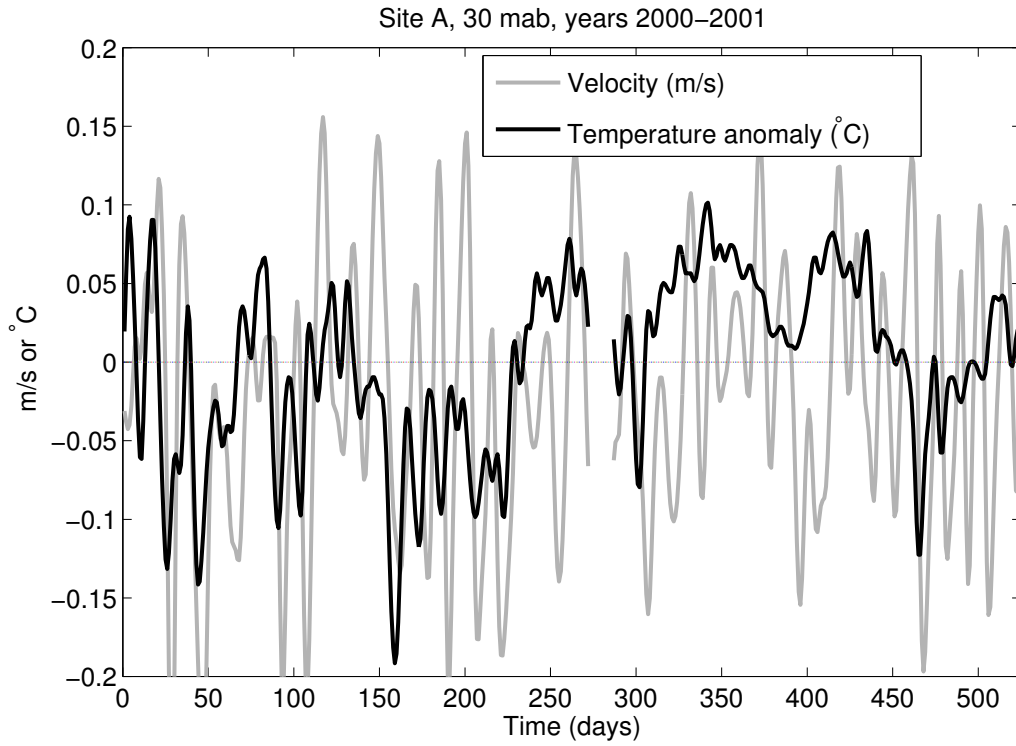


Fig. 9. Filtered time series of the velocity in the direction of the bathymetric contours, and the temperature anomaly relative to the mean ( $4.22^{\circ}$ ). The data are from the first two current meter deployments (from March 2000 to September 2001) at 30 mab at site A.

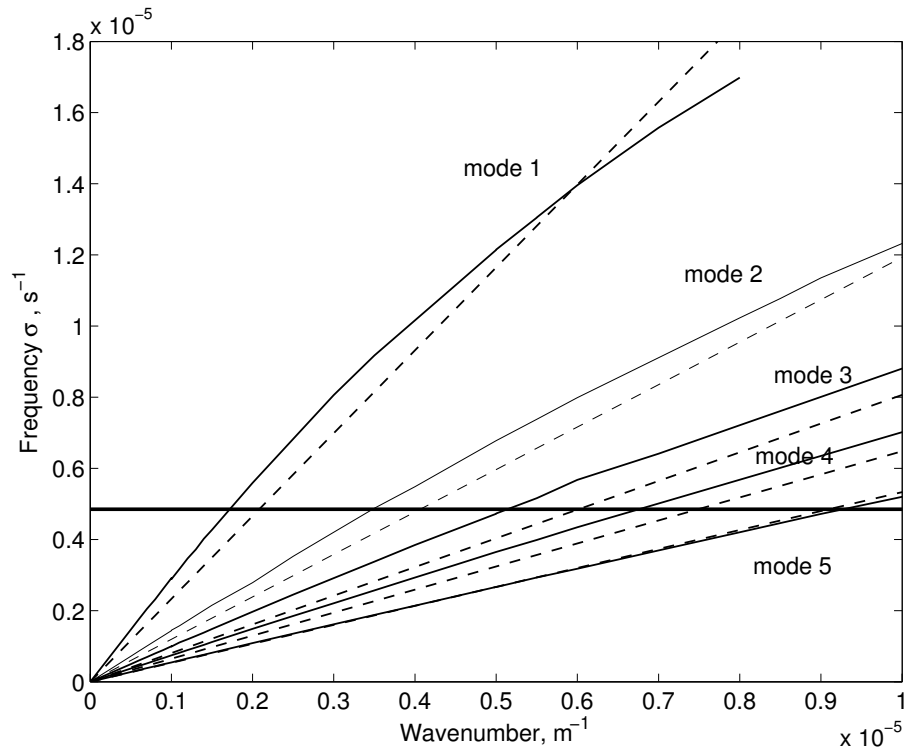


Fig. 10. Dispersion relation for the first 5 modes of coastal trapped waves in the BIOZAIRE area (solid curves). For each mode, the dashed line represents the dispersion relation of a flat bottom Kelvin wave (4000 m depth). The period  $2\pi/\sigma = 15$  days is indicated by a horizontal line.

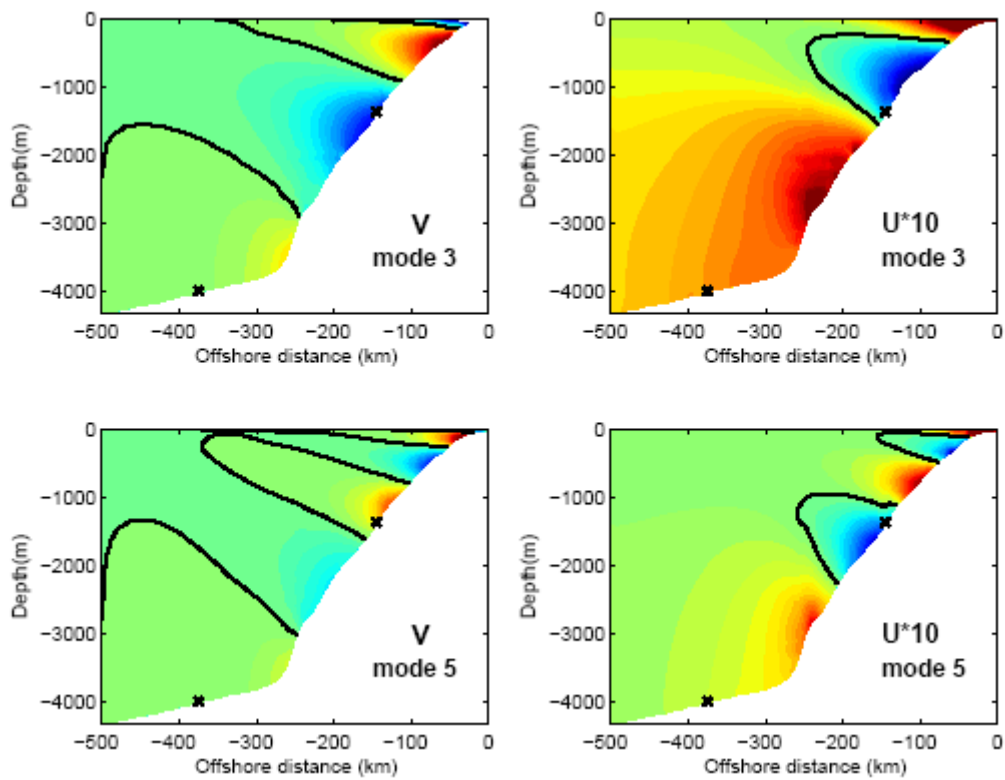


Fig. 11. Spatial structure of the perturbation of along-shore velocity  $V$  and cross-shore velocity  $U$  for coastal trapped wave modes 3 and 5. Velocities are rescaled so that the maximum of is one; note that is multiplied by 10 to be plotted with the same color scale. The zero contour is indicated by the thick line. Crosses indicate the location of mooring C (near 4000 m) and mooring A (near 1300 m).

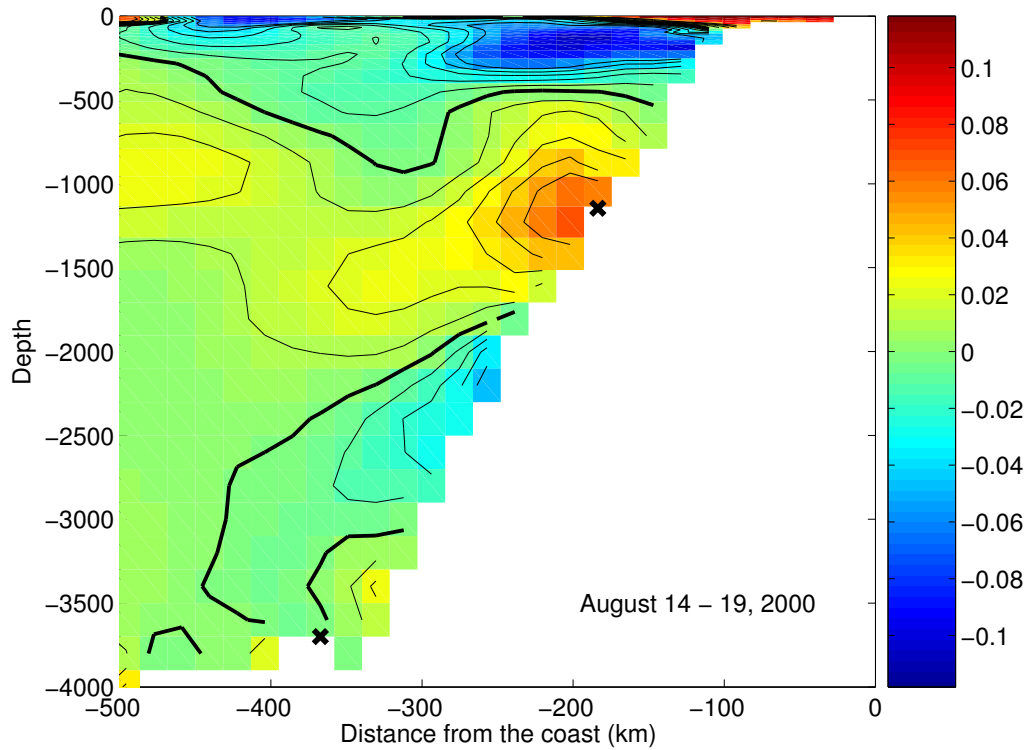


Fig. 12. Meridional velocity at  $7.3^{\circ}\text{S}$  in the ATL6 model ( $\text{m/s}$ ), averaged over 5 days (14-19 August 2000). Each colored box is a model grid cell. Contours are from  $-0.05 \text{ m.s}^{-1}$  to  $0.05 \text{ m.s}^{-1}$  by  $0.01 \text{ m.s}^{-1}$ . The zero contour is indicated in bold. Black crosses note the approximate location of moorings A and C.

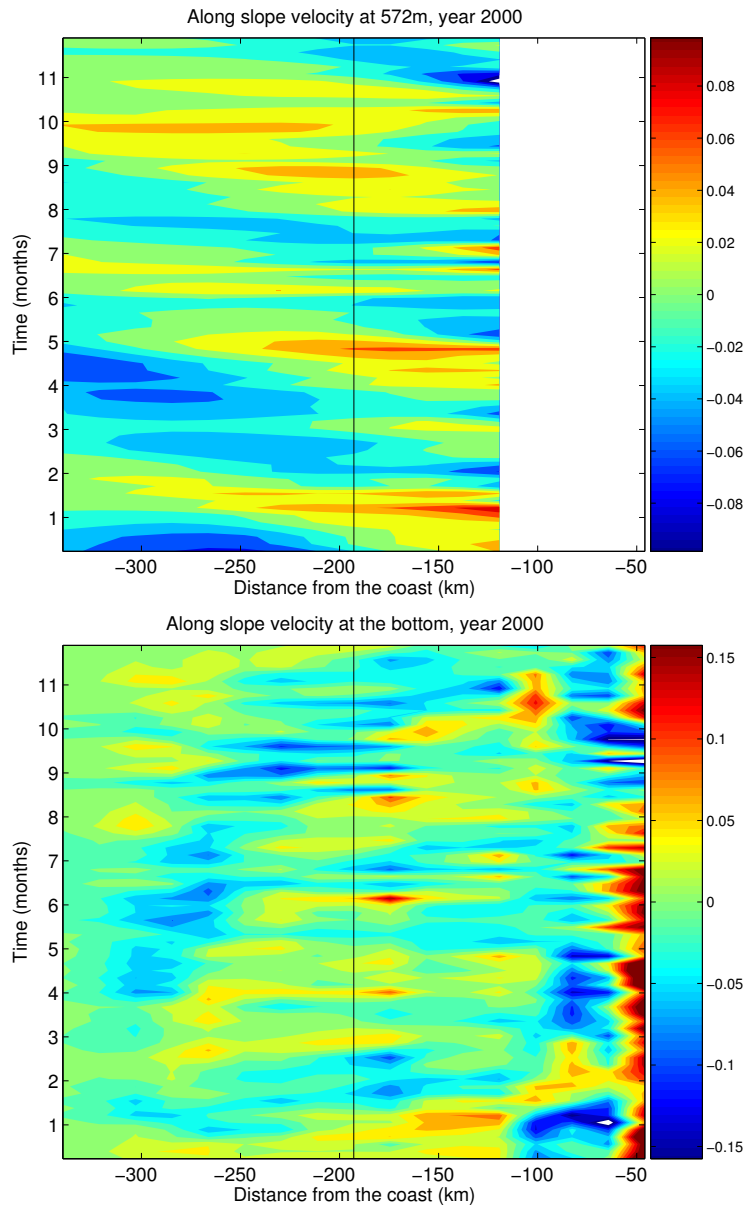


Fig. 13. Time-series of meridional velocity along the slope at  $7.3^{\circ}\text{S}$  in the ATL6 model (m/s), for year 2000, from the 5-days averaged model output. A black line is drawn at the approximate location of site A (site C is at the western boundary of the plot). Top panel: velocity in model layer 17 (572 m depth). Bottom: velocity in the model bottom layer.